DE GRUYTER
OPEN

Atomic short-range order in mechanically synthesized iron based Fe-Zn alloys studied by ^{57}Fe Mössbauer spectroscopy

Robert Konieczny,
Rafał Idczak

Abstract. Mechanical alloying method was applied to prepare nanocrystalline iron-based $Fe_{1-x}Zn_x$ solid solutions with x in the range $0.01 \leq x \leq 0.05$. The structural properties of the materials were investigated with the Mössbauer spectroscopy by measuring the room temperature spectra of ^{57}Fe for as-obtained and annealed samples. The spectra were analyzed in terms of parameters of their components related to unlike surroundings of the iron probes, determined by different numbers of zinc atoms existing in the neighborhood of iron atoms. The obtained results gave clear evidence that after annealing process, the distribution of impurity atoms in the first coordination spheres of ^{57}Fe nuclei is not random and it cannot be described by binomial distribution. The estimated, positive values of the short-range order parameters suggest clustering tendencies of Zn atoms in the Fe-Zn alloys with low zinc concentration. The results were compared with corresponding data derived from Calphad calculation and resulting from the cellular atomic model of alloys by Miedema.

Key words: hyperfine interactions • mechanical alloying • Mössbauer spectroscopy • nanocrystalline materials • short-range order

Introduction

Mechanical alloying (MA) is one of the non--equilibrium processing methods [1] that allow one to obtain such materials as nanocrystalline solid solutions, amorphous alloys, or composites with unique properties. The controlled thermal treatment of mechanically alloyed products combined with a structural investigation, allow determining the structural stability of the materials. Monitoring of MA by Mössbauer spectroscopy concerns important information about structural changes, phase transformations, magnetic and thermodynamic properties.

While the macroscopic magnetic properties of the binary iron-based alloys obtained by various methods were described in the literature quite well, the hyperfine interactions in these alloys are not well known, especially in the case of the mechanically synthesized alloys being subsequently subjected to thermal treatment. Moreover it is known that mechanical, magnetic, and thermodynamic properties of alloys depend, in general, on local fluctuations in their composition. These fluctuations can be quantitatively described in terms of the short-range order (SRO) parameter α, introduced by Cowley [2]. Physically, this parameter measures the deviation at short range from the random state, with values

R. Konieczny✉, R. Idczak
Institute of Experimental Physics,
University of Wrocław,
9 M. Borna Sq., 50-204 Wrocław, Poland,
Tel.: +48 71 375 9336, Fax: +48 71 328 7365,
E-mail: robi@ifd.uni.wroc.pl

from $1 - 1/x$ to 1; 0 corresponds to the random state whereas x is a fraction of impurity atoms dissolved in the alloy. For this reason, in recent years many theoretical [3–6] and experimental [7–11] studies have been made to a better understanding of the atomic ordering arises on alloying and further heat treatment.

The aim of this work was to apply the ^{57}Fe Mössbauer spectroscopy for determination of hyperfine interactions and the local atomic order in nanocrystalline Fe-Zn alloys mechanically alloyed and then thermally annealed. It is worth noticing that the values of the SRO parameter obtained from such a study are related to the distribution of impurity atoms in the nearest neighbor shells of the ^{57}Fe Mössbauer probe and the distribution depends on the type of interaction between impurity and iron atoms.

Experimental and results

The powder samples of $Fe_{1-x}Zn_x$ alloys with x in the range $0.01 \le x \le 0.05$, were prepared by milling appropriate amounts of the Aldrich 99.98% pure crystalline iron and 99.999% pure crystalline zinc; both materials in a form of particles with sizes less than 0.5 mm. The mechanical alloying processes were performed in a Fritsch Pulverisette 6 planetary ball mill with stainless-steel vial and balls. The total weight of the powders was 10 g and the ball-to-powder weight ratio was 10:1. The milling processes were carried out at room temperature under an argon atmosphere and the milling speed amounted to 500 rpm.

The room temperature ^{57}Fe Mössbauer spectra were measured for the studied samples by means of a constant-acceleration POLON spectrometer of standard design. The measurements for each specimen were performed twice, just after its synthesis in the mill and after an annealing process. All samples were annealed in vacuum at 700 K for 12 h. After that they were slowly cooled to room temperature over 6 h. Under these conditions, diffusion effectively stops at a certain temperature T_d, so the observed distributions of atoms in the annealed specimens should be the frozen-in state, corresponding to the temperature. According to the data given in the literature, T_d for iron is close to 700 K [12]. Spectra for the samples after the annealing process are presented in Fig. 1.

Each measured spectrum was fitted with a sum of a certain number of different six-line patterns corresponding to hyperfine fields (B) at ^{57}Fe nuclei generated by different numbers of Fe and Zn atoms located in the first coordination shell of the probing nuclei. The number of fitted patterns depended on the concentration of zinc in the samples. The fitting procedure was done under assumption that the influence of Zn atoms on B as well as the corresponding isomer shift (IS) of a six-line subspectrum, are additive and independent of the atom positions in the first coordination shell of the nuclear probe [13]. In other words it was accepted that for each
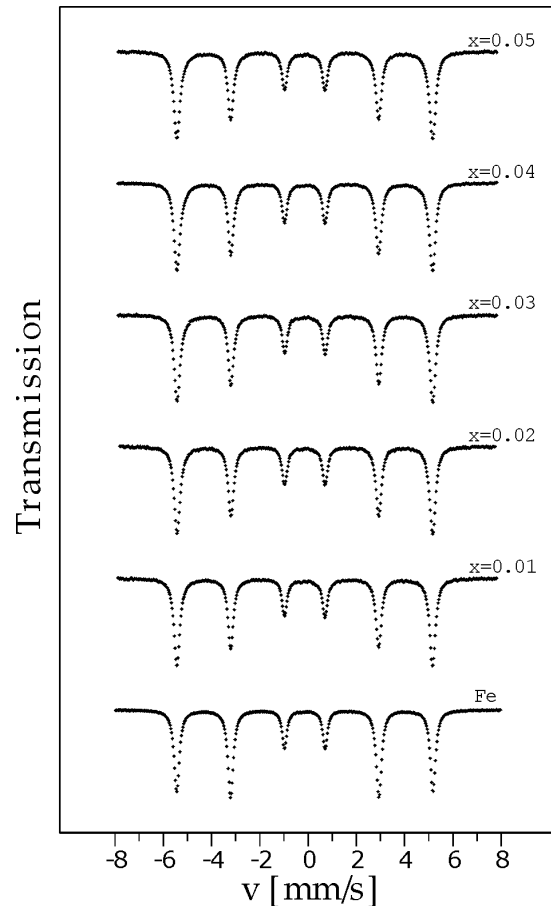

Fig. 1. The ^{57}Fe Mössbauer spectra for the nanocrystalline $Fe_{1-x}Zn_x$ alloys measured at room temperature after the annealing process at 700 K.

subspectrum the quantities B and IS are linear functions of the numbers n of Zn atoms located in the first coordination shell of ^{57}Fe and the functions can be written as follows:

$$(1) \qquad \begin{aligned} B(n) &= B_0 + n\Delta B_1 \\ IS(n) &= IS_0 + n\Delta IS_1 \end{aligned}$$

where ΔB_1 (ΔIS_1) stands for the change of B (IS) with one Zn atom located in the first coordination shell of the Mössbauer probe. At the same time we assume that the quadrupole splitting/shift QS for all fitted six-line patterns is equal to zero because of the cubic symmetry of the iron-based alloys. Moreover, it was assumed that the three linewidths Γ_{16}, Γ_{25} and Γ_{34} for all components of a spectrum which are related to the existence of impurity atoms in the first coordination shell of ^{57}Fe are the same and they are different from linewidths of that component, determined by the nuclear probes having in their vicinity only Fe atoms. This division of sub spectra into two sets with different linewidths takes into account the fact observed for other systems, that the linewidths can be influenced by an existence of large/small enough impurity atoms in the nearest neighborhood of the Mössbauer probes. The example of a fit obtained under these assumptions is presented in Fig. 2 whereas the found values of the best-fit parameters are displayed in Table 1. The values essentially differ from corresponding data
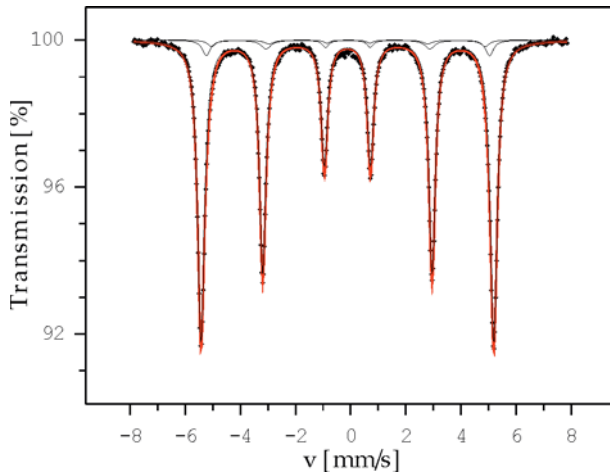
Fig. 2. The ^{57}Fe Mössbauer spectrum for the $Fe_{0.95}Zn_{0.05}$ alloy measured at room temperature after the annealing process at 700 K, fitted with three six-line subspectra.

given in the literature [14–16]. In Ref. [14] one can find that for the $Fe_{0.965}Zn_{0.035}$ alloy $B_0 = 32.96(2)$ T, $\Delta B_1 = -1.60(2)$ T, $\Delta B_2 = -0.06(3)$ T, $\Delta B_3 = 1.30(2)$ T, and for $Fe_{1-x}Zn_x$ ($x < 0.2$) [15]: $\Delta B_1 = -1.80$ T, $\Delta B_2 = -0.70$ T. At the same time, theoretically calculated values reported in work [16] are $\Delta B_1 = -1.34$ T, $\Delta B_2 = -0.28$ T, $\Delta B_3 = 0.74$ T.

As the main result of the analysis, the values of parameters $c(0)$, $c(1)$, and $c(2)$ were determined. The parameters are intensities of those components of a spectrum which are related to the existence of zero, one or two (n) zinc atoms in the first coordination shell of nuclear probes ^{57}Fe, respectively. The $c(n)$ values were used to find parameter $<n>$ being the average number of Zn atoms in the first coordination shell of ^{57}Fe Mössbauer probe:

$$(2) \qquad \langle n \rangle = \sum_{n=1}^{8} nc(n)$$

The results are presented in Figs. 3a and 3b.

In disordered iron-based alloys, the probability $p(n)$ of occurring given configuration of impurity atoms in the first coordination spheres of ^{57}Fe nucleus can be described by the binomial distribution $p(n) = [N!/((N-n)!n!)]x^n(1-x)^{N-n}$ where N denotes, for example, the coordination number of the first or first and second spheres, x is the concentration of impurity atoms, and n stand for the number of impurity atoms in the first or the first and second coordination spheres. In the case of $Fe_{1-x}Zn_x$ alloys with the x range $0.01 \leq x \leq 0.05$, atoms are distributed in the bcc lattice and the total number of atoms located in first coordination sphere of ^{57}Fe
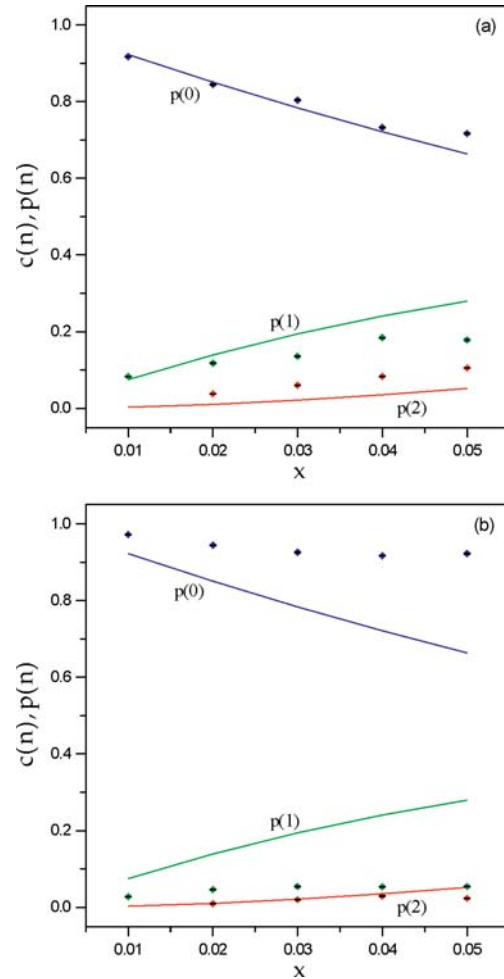

Fig. 3. Total intensities of those components of a spectrum which are related to the existence of zero ($c(0)$ blue points), one ($c(1)$ green points) and two ($c(2)$ red points) Zn atoms in the first coordination shells of nuclear probes ^{57}Fe in the nanocrystalline $Fe_{1-x}Zn_x$ alloys after (a) the mechanical milling and (b) the annealing process at 700 K. The solid lines describe probabilities of finding zero $p(0)$, one $p(1)$ and two $p(2)$, Zn atoms in the first coordination shell ($N_1 = 8$) of an Fe atom in the random bcc $Fe_{1-x}Zn_x$ alloy.

is equal to 8. In the real alloys, the distribution of impurity atoms is generally different from the statistical one. This deviation from the random state can be quantitatively described by SRO parameter. The SRO parameters for systems with bcc lattice have the following form [2]:

$$(3) \qquad \alpha_1 = 1 - \frac{\langle n \rangle}{8x}$$

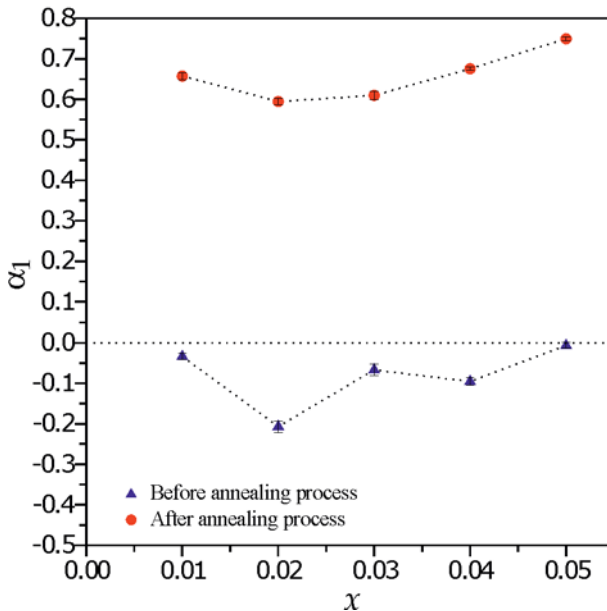when it concerns the first coordination shell.

Table 1. Some of the best-fit parameters of the assumed model of the ^{57}Fe Mössbauer spectrum measured for annealed samples of $Fe_{1-x}Zn_x$ alloys. The standard uncertainties for the parameters result from the variance of the fit

x	B_0 [T]	ΔB_1 [T]	IS_0 [mm/s] (relative to α-Fe)	ΔIS_1 [mm/s]
0.01	32.898(46)	−0.963(16)	0.0087(29)	0.0016(11)
0.02	32.889(48)	−1.067(13)	0.0070(21)	0.0081(37)
0.03	32.905(71)	−0.884(12)	0.0085(26)	0.0090(39)
0.04	32.886(41)	−1.021(15)	0.0075(35)	0.0225(30)
0.05	32.916(51)	−1.066(17)	0.0075(39)	0.0181(52)

Table 2. The SRO parameter α_1 for the nanocrystalline $Fe_{1-x}Zn_x$ alloys deduced from the ^{57}Fe Mössbauer spectra

x	Powder samples before annealing process α_1	Powder samples after annealing process α_1
0.01	−0.0338(74)	0.6573(86)
0.02	−0.2070(14)	0.5948(78)
0.03	−0.0670(13)	0.6100(10)
0.04	−0.0956(91)	0.6492(36)
0.05	−0.0064(58)	0.7497(55)

Basing on the intensities of the spectrum components $c(n)$, we determined the short-range order (SRO) parameter α_1 [2, 10] which describes the deviation from the random distribution of atoms being in the first coordination shell of the nuclear probes. The values of α_1 were determined for two kinds of samples, those as-obtained in a planetary ball mill as well as those annealed at 700 K for 12 h. The results are presented in Table 2 and Fig. 4. As one can see for all as-obtained specimens the α_1 parameter is negative and its absolute value is relatively small. This testifies that the Zn atoms were practically randomly distributed in the iron matrix during the mechanical alloying process. On the other hand in the case of the annealed samples the situation is different because one observes positive large values of α_1. The α_1 values suggest that in the first shell of the nuclear probes being in the annealed alloys there are much less Zn atoms than in corresponding random alloys. The fact can be explained by a tendency of Zn atoms to form clusters in iron-based Fe-Zn solid solutions on annealing. In terms of interactions it means that the interaction between Fe and Zn atoms

is repulsive (predominance of Zn-Zn bonds). The observation can be compared with the Miedema's model predictions [17] on the enthalpy H_{Fe-Zn} of the solution of Zn in Fe as well as the results of Calphad calculations concerning enthalpy of formation H^{for} for the Fe-Zn alloys [18–20]. It is possible because the enthalpy H^{for} is related to the enthalpy H_{Fe-Zn} in the following way:

$$(4) \qquad H_{Fe-Zn} = [dH^{for}/dx]_{x=0}$$

On the other hand, the enthalpy H_{Fe-Zn} is related to the binding energy E_b between two Zn atoms in the dilute $Fe_{1-x}Zn_x$ system with x close to zero. According to Królas model [21]

$$(5) \qquad H_{Fe-Zn} = -z \cdot E_b(0)/2,$$

where $E_b(0)$ is the extrapolated value of E_b for $x = 0$ and z stands for the coordination number of the crystalline lattice ($z = 8$ for α-Fe).

Positive value of enthalpy H_{Fe-Zn} of solution of zinc in iron predicted by Miedema's model (displayed in Table 3) means that interaction between zinc atoms in iron matrix is attractive – negative value of binding energy between two Zn atoms. This model prediction coincides with our observation based on SRO values, that zinc atoms form clusters in iron-based Fe-Zn solid solutions. However, Calphad calculations are at variance with such result. Negative values of enthalpy H_{Fe-Zn} of solution of zinc in iron obtained on the basis of Calphad computations (included in Table 3) indicate that the interaction between zinc atoms is repulsive – positive value of binding energy between two Zn atoms.

Fig. 4. SRO parameter α_1 as a function of fraction x of Zn atoms in the nanocrystalline $Fe_{1-x}Zn_x$ alloys.

Table 3. The enthalpy H_{Fe-Zn} [eV/atom] of solution of zinc in iron

Miedema's model [17]	Calphad computations [18*, 19**, 20***]
1.183	−0.059*, −0.065**, −0.088***

Conclusions

The ^{57}Fe Mössbauer study of the short-range order parameter α_1 for $Fe_{1-x}Zn_x$ nanocrystalline alloys reveals that the parameter depends on the heat treatment of the investigated specimens. For the as-obtained powder specimens, the α_1 parameters are negative and its absolute value is relatively small. This testifies that the Zn atoms were practically randomly distributed in the iron matrix during the mechanical alloying process. On the other hand in the case of the annealed samples, the situation is different because one observes disappearance of the slight ordering-type correlations (the predominance of Fe-Zn bonds) and nanocrystalline alloy exhibits clustering tendencies. The positive α_1 value means that in the first coordination shell of the nuclear

probes being in the annealed nanocrystalline alloys, there are much less Zn atoms than in corresponding random alloys. In terms of interactions it means that the interaction between two Zn atoms is attractive (predominance of Zn-Zn bonds). This conclusion agrees with the semi-empirical Miedema's model predictions [17] and it is at variance with Calphad calculations [18–20].

References

1. Suryanarayana, C. (2001). Mechanical alloying and milling. *Prog. Mater. Sci.*, *46*, 1–184. DOI: 10.1016/S0079-6425(99)00010-9.

2. Cowley, J. M. (1950). An approximate theory of order in alloys. *Phys. Rev.*, *77*, 669–675. DOI: 10.1103/PhysRev.77.669.

3. Staunton, J. B., Ling, M. F., & Johnson, D. D. (1997). A theoretical treatment of atomic short-range order and magnetism in iron-rich b.c.c. alloys. *J. Phys.-Condens. Matter*, *9*, 1281–1300. DOI: 10.1088/0953-8984/9/6/014.

4. Erhart, P., Caro, A., Serrano de Caro, M., & Sadigh, B. (2008). Short-range order and precipitation in Fe-rich Fe-Cr alloys. *Phys. Rev. B*, *77*, 134206–134214. DOI: http://dx.doi.org/10.1103/PhysRevB.77.134206.

5. Bonny, G., Erhart, P., Caro, A., Pasianot, R. C., Malerba, L., & Caro, M. (2009). The influence of short range order on the thermodynamics of Fe-Cr alloy. *Model. Simul. Mater. Sci. Eng.*, *17*, 025006–025021. DOI: 10.1088/0965-0393/17/2/025006.

6. Gorbatov, O. I., Kuznetsov, A. R., Gornostyrev, Yu. N., Ruban, A. V., Ershov, N. V., Lukshina, V. A., Chernenkov, Yu. P., & Fedorov, V. I. (2011). Role of magnetism in the formation of a short-range order in iron-silicon alloys. *J. Exp. Theor. Phys.*, *112*, 848–859. DOI: 10.1134/S1063776111040066.

7. Mirebeau, I., & Parette, G. (2010). Neutron study of the short range order inversion in Fe$_{1-x}$Cr$_x$. *Phys. Rev. B*, *82*, 104203–104208. DOI: 10.1103/PhysRevB.82.104203.

8. Jartych, E. (2003). Local atomic order in nanocrystalline Fe-based alloys obtained by mechanical alloying. *J. Magn. Magn. Mater.*, *265*, 176–188. DOI: 10.1016/S0304-8853(03)00263-4.

9. Dubiel, S. M., & Cieślak, J. (2013). Effect of thermal treatment on the short-range order in Fe-Cr alloys. *Mater. Lett.*, *107*, 86–89. DOI: 10.1016/j.matlet.2013.05.127.

10. Idczak, R., Konieczny, R., & Chojcan, J. (2013). Short-range order in iron alloys studied by ^{57}Fe Mössbauer spectroscopy. *Solid State Commun.*, *159*, 22–25. DOI: 10.1016/j.ssc.2013.01.015.

11. Idczak, R., Konieczny, R., & Chojcan, J. (2012). Atomic short-range order in Fe$_{1-x}$Cr$_x$ alloys studied by ^{57}Fe Mössbauer spectroscopy. *J. Phys. Chem. Solids*, *73*, 1095–1098. DOI: 10.1016/j.jpcs.2012.05.010.

12. Idczak, R., Konieczny, R., & Chojcan, J. (2012). An enthalpy of solution of chromium in iron studied with ^{57}Fe Mössbauer spectroscopy. *Physica B*, *407*, 2078–2081. DOI: 10.1016/j.physb.2012.02.009.

13. Vincze, I., & Campbell, I. A. (1973). Mössbauer measurements in iron base alloys with transition metals. *J. Phys. F*, *3*, 647–663. DOI: 10.1088/0305-4608/3/3/023.

14. Błachowski, A., Ruebenbauer, K., Żukrowski, J., Przewoźnik, J., Marzec, J., & Rakowska, A. (2011). Spin- and charge density perturbations and short-range order in Fe-Cu and Fe-Zn BCC alloys: A Mössbauer study. *J. Phys. Chem. Solids*, *72*, 1537–1542. DOI: 10.1016/j.jpcs.2011.08.032.

15. Laggoun, A., Hauet, A., & Teillet, J. (1990). Mössbauer study of Zn effect on bcc iron in metastable Fe-Zn alloys. *Hyperfine Interact.*, *54*, 825–829. DOI: 10.1007/BF02396136.

16. Błachowski, A., & Wdowik, U. D. (2012). Transition metal impurity effect on charge and spin density in iron: Ab initio calculations and comparison with Mössbauer data. *J. Phys. Chem. Solids*, *73*, 317–323. DOI: 10.1016/j.jpcs.2011.10.017.

17. Miedema, A. R. (1992). Energy effects and charge transfer in metal physics, modeling in real space. *Physica B*, *182*, 1–17. DOI: 10.1016/0921-4526(92)90565-A.

18. Xiong, W., Kong, Y., Du, Y., Liu, Z. K., Selleby, M., & Sun, W. (2009). Thermodynamic investigation of the galvanizing systems, I: Refinement of the thermodynamic description for the Fe-Zn system. *Computer Coupling of Phase Diagrams and Thermochemistry*, *33*, 433–440. DOI: 10.1016/j.calphad.2009.01.002.

19. Su, X., Tang, N., & Toguri, J. M. (2001). Thermodynamic evaluation of the Fe-Zn system. *J. Alloy. Compd.*, *325*, 129–136. DOI: 10.1016/S0925-8388(01)01273-7.

20. Nakano, J., Malakhov, D. V., & Purdy, G. R. (2005). A crystallographically consistent optimization of the Zn-Fe system. *Computer Coupling of Phase Diagrams and Thermochemistry*, *29*, 276–288. DOI: 10.1016/j.calphad.2005.08.005.

21. Królas, K. (1981). Correlation between impurity binding energies and heat of formation of alloys. *Phys. Lett. A*, *85*, 107–110. DOI: 10.1016/0375-9601(81)90235-8.